Dalton Transactions

Accepted Manuscript

ROYAL SOCIETY OF CHEMISTRY

www.rsc.org/dalton

Design and synthesis of BODIPY-Clickates based Hg^{2+} sensors: Effect of triazole binding mode with Hg^{2+} on signal transduction

Mani Vedamalai,[a] Dhaval Kedaria,[b] Rajesh Vasita,[b] Shigeki Mori[c] and Iti Gupta[a,*]

[a,*]Indian Institute of Technology Gandhinagar, VGEC Campus, Chandkheda, Ahmedabad-382424, India.
[b] School of Life Sciences, Central University of Gujarat, Gandhinagar, Gujarat, India.
[c] Integrated Centre for Sciences, Ehime University, Matsuyama, 790-8577, Japan.

Abstract

BODIPY-Clickates, **F1** and **F2**, for the detection of Hg^{2+} have been designed, synthesized and characterized. Both **F1** and **F2** showed hyperchromic shifts in the UV-visible spectra in response to increasing Hg^{2+} concentrations. Hg^{2+} ion binding caused perturbation of emission quenching process and chelation induced enhanced bathochromic emission of **F1** and **F2** to 620 nm and 660 nm, respectively. Job plot clearly indicated that binding ratio of **F1** and **F2** with Hg^{2+} was 1:1. The NMR titration of BODIPY-clickates with Hg^{2+} confirmed that aromatic and triazole were involved in the binding event. Furthermore, HRMS data of **F1-Hg^{2+}** and **F2-Hg^{2+}** supported the formation of mercury complexes of BODIY-Clickates. Dissociation constant for the interaction between fluorescent probes **F1** and **F2** with Hg^{2+} was found to be 24.4 ± 5.1 µM and 22.0 ± 3.9 µM, respectively. Hg^{2+} ion induced fluorescence enhancement was almost stable in a pH range of 5 to 8. Having less toxicity to live cells, both the probes were successfully used to map the Hg^{2+} ions in live A549 cells.

Keywords: BODIPY-Clickates, Mercury-sensing, Fluorescent probes, Bioimaging, Crystal structure

Introduction

There is a great demand for novel fluorescent probes in the detection of heavy metal ions owing to their toxicity to living systems. Among these, mercury is known to be neuro toxin due its high affinity towards thiols and amino groups in peptides and nucleic acids, leading to many health problems such as kidney failure, brain damage, myocardial infarction, acrodynia, Minamata disease, cognitive and motion disorders.[1] Fluorescence sensing has been more attractive area of research over other branches due to its versatile application in bio labelling, pathological process, metal ion sensing, disease diagnostic,

industrial products, environmental pollutants and drug delivery system.[2] It does not need any highly sophisticated instruments, tedious sample preparation, and pre-treatment. In particular, organic fluorescent dyes have been extensively used as signaling moiety owing to their high sensitivity, brightness, tuneable photo physical properties, cheap starting materials, easy to conjugate with biomolecules and nanomaterials. Turn-on fluorescent probes for Hg^{2+} is scarce owing to the large spin-orbit coupling which activates non-radiative transition.[3] Over a last decade, paramount efforts have been laid on BODIPY dye based fluorescent reporters because of its versatile nature in synthesis of derivatives, high molar absorption coefficient, high photo stability, and high quantum yield.[4] Most of the metal ion sensing fluorescent probes commonly use Schiff base, thio ether, crown ether, triazole, pyridine, quinoline, cyclam, and aromatic amine as a recognizing moiety wherein metal ion recognition enhances contrast between metal ion bound fluorophore and metal ion free fluorophore.[5] *meso* anilino appended BODIPY probes are an ideal platform for sensing metal ions on the basis of either photo-induced electron transfer or intramolecular charge transfer (ICT). Incorporation of N-heterocyclic recognition units such as pyridine,[6] quinoline,[7] triazole,[8] and aromatic imine[9] generate strong emission by chelation induced enhance fluorescence (CHEF) because of reversal of n-π* to π-π* transition. Polar solvents induced twisted intramolecular charge transfer (TICT) is well known in aniline analogous attached fluorophore in which rotation of C-N linkage influences charge separation between donor and acceptor.[10] Metal induced TICT based fluorescent probes are very rare and the mechanism is complicated.[11] Triazole has been extensively used to design metal ion responsive fluorescent probes as they can recognize the metal ions due to presence of multiple nitrogens.[12] In general, triazoles are synthesized by Cu(I) catalyzed click chemistry reaction between alkyne and azide[13] and largely used in synthesis of dendrimers,[14] metal organic frameworks,[15] fluorescent probes,[16] biomolecule conjugates,[17] and nanomaterial-organic conjugates.[18] The objective of this work is to evaluate the prospective of Hg^{2+} chelation on signal transduction process. Recently, triazole functionalized BODIPY derivatives have been successfully used for the detection of Hg^{2+} ions in both organic and buffered medium and emit the green emission upon binding with Hg^{2+} with small Stokes shift.[19] In our strategy, triazole

functionalized BODIPY is emitting at red region upon binding with Hg^{2+} with large Stokes shift due to charge transfer state.

Experimental section:

Synthetic materials and methods

All the chemicals and reagents were used without purification as obtained, unless or otherwise mentioned. Chloroform-d (99.8 atom % D and 0.03 % TMS), 2, 3-Dichloro-5,6-dicyno- 1,4-benzoquinone, HEPES, $AgNO_3$ $CaCl_2.2H_2O$, and $ZnSO_4.H_2O$ were purchased from Sigma Aldrich, India. Triethylamine, dimethylformamide, $CdCl_2.H_2O$, $CuSO_4.5H_2O$, $FeSO_4.7H_2O$, $FeCl_3$ and acetonitrile were obtained from Merck Pvt. Ltd., India. Sodium azide, boron trifluoride diethyl etherate, phenyl acetylene, sodium ascorbate, 1-heptyne, dimethyl sulfoxide – d6 (99.8 atom % D) and $Hg(ClO_4)_2.3H_2O$ were procured from Acros Organics. Aniline, trifluoroacetic acid, tetrabutylammonium bromide, K_2CO_3, HCl, NaOH, $CoCl_2.6H_2O$, KCl, $MgSO_4.7H_2O$, $MnSO_4.H_2O$, $Ni(CH_3CO_2)_2$ and $Pb(NO_3)_2$ were obtained from S. D. Fine Chem. Ltd., India. 2-Chloroethanol, pyrrole, and phosphorous oxychloride were obtained from SpectroChem Pvt. Ltd., India. Dichloromethane, hexane, and methanol were supplied by Merck Pvt. Ltd. for silica gel column chromatographic purification. Spectroscopic grade solvents were procured from S. D. Fine Chem. Ltd., India.

Instrumentation

NMR spectra of organic compounds were recorded with a Bruker Avance III 500 MHz NMR spectrometer at 24°C. The HRMS measurement for all the compounds were recorded (in positive ion mode) with Waters Synapt-G2S ESI-Q-TOF Mass instrument. UV-visible absorption measurements were recorded with Shimadzu UV-1700 and fluorescence emission studies were done using a Horiba-Jobin Yvon Fluolorog-3 Spectrometer (Ex. slit width/Em. slit width = 3 nm). Thermo Scientific™ water purification system (TKA, Germany) was used to deionize water.

Synthesis of compound 1

Compound **1** had been synthesized according to the already reported synthetic procedure.[20]

Synthesis of 4-(di (1H-pyrrol-2-yl) methyl)-N, N-bis (2-chloroethyl) benzenamine (2)

A mixture of compound **1** (416.5 mg, 1.7 mmol) and pyrrole (1.2 mL, 17 mmol) was treated with trifluoroacetic acid (0.1 mL) for 1 hour. Then, reaction mixture was quenched with dilute sodium bicarbonate solution and dried over anhydrous sodium sulphate. Organic solvents were evaporated under vacuum and the crude product was purified on silica gel column chromatography using dichloromethane and hexane (1:4, v/v) as an eluent mixture. White colored solid was obtained (Yield 437.0 mg, 71%). HRMS ESI calculated for $C_{19}H_{22}Cl_2N_3$ $[M+H]^+$: 362.1191; found: 362.1187. ^{1}H NMR ($CDCl_3$, 500 MHz): δ = 7.93 (s, 2H), 7.10 (d, J = 9.0 Hz, 2H), 6.69 (dd, J = 2.5, 4.0, 2H), 6.63 (d, J = 9.0 Hz, 2H), 6.16 (dd, J = 3.0, 6.0 Hz, 2H), 5.92 (s, 2H), 5.39 (s, 1H), 3.71 (t, J = 7.0 Hz, 4H), 3.62 (t, J = 6.5 Hz, 4H). ^{13}C NMR ($CDCl_3$, 125 MHz): δ = 145.0, 132.91, 131.2, 129.6, 117.0, 112.0, 108.4, 106.9, 53.5, 42.9, 40.4.

Synthesis of 4, 4-difluoro-8-[N, N-bis (2-chloroethyl) benzenamino]-4- bora-3a, 4a-diaza-*s*-indacene (3)

A 25 mL solution of 2, 3-Dichloro-5, 6-dicyano-1, 4-benzoquinone (227.0 mg, 1.0 mmol) in dry dichlormethane was added to 100 mL round bottom flask containing compound **2** (290.0 mg, 0.8 mmol) in dry dichloromethane (10 mL) and stirred for 2 hours. Then, reaction mixture was treated with trimethylamine (2 mL) and followed by boron trifluoride diethyl etherate (3 mL) for overnight. The reaction mixture was washed with dilute sodium bicarbonate solution (X 3) and dried over anhydrous sodium sulphate. Organic solvents were removed utilizing rotatory evaporator and purified on silica gel column chromatography using dichloromethane and hexane as an eluent (10:1, v/v). Orange colored organic layer was collected and dried in rotary evaporation (Yield 231.7 mg, 71%). HRMS ESI calculated for $C_{19}H_{19}BCl_2F_2N_3$ $[M+H]^+$: 408.1017; found: 408.1009. ^{1}H NMR ($CDCl_3$, 500 MHz): δ = 7.90 (s, 2H), 7.56 (d, J = 9.0 Hz, 2H), 7.02 (d, J = 3.5 Hz, 2H), 6.82 (d, J = 9 Hz, 2H), 6.55 (d, J = 2.5 Hz, 2H), 3.87 (t, J = 7 Hz, 4H),

3.73 (t, J = 7.0 Hz, 4H). ^{13}C NMR ($CDCl_3$, 125 MHz): δ = 148.8, 147.6, 142.5, 134.5, 133.2, 130.9, 123.1, 117.9, 111.5, 53.3, 40.1.

Synthesis of 4,4-difluoro-8-[N, N-bis (2-azidoethyl) benzenamino]-4-bora-3a,4a-diaza-*s*-indacene (4)

Sodium azide (325.0 mg, 2 mmol), tetrabutyl ammonium bromide (32.2 mg, 0.1 mmol) and compound **3** (163.2 mg, 0.4 mmol) were dissolved in dry acetonitrile and refluxed for 24 hours. Then, reaction mixture was brought to room temperature and acetonitrile was removed under vacuum. Crude product was extracted with dichloromethane and washed with deionized water. Organic layer was dried over anhydrous sodium sulphate and removed using vacuum evaporator. Crude product was purified on silica gel column chromatography using dichloromethane and hexane (5:1, v/v) as an eluent mixture. Rotary evaporation of the organic phase afforded **4** as orange colored solid. (Yield obtained 128.3 mg, 76%). HRMS ESI calculated for $C_{19}H_{19}BF_2N_9$ $[M+H]^+$: 422.1825; found: 422.1813. ^{1}H NMR ($CDCl_3$, 500 MHz): δ = 7.90 (s, 2H), 7.56 (d, J = 9.0 Hz, 2H), 7.04 (d, J = 4.0 Hz, 2H), 6.83 (d, J = 8.5 Hz, 2H), 6.55 (d, J = 2.5 Hz, 2H), 3.70 (t, J = 6.0 Hz, 4H), 3.61(t, J = 6.0 Hz, 4H). ^{13}C NMR ($CDCl_3$, 125 MHz): δ = 149.0, 147.7, 142.4, 134.5, 130.9, 123.1, 117.9, 111.7, 50.6, 48.7.

Synthesis of 4, 4-difluoro-8-[N, N-bis (2-(4-pentyl-1H-1, 2, 3-triazol-1-yl) ethyl) benzenamino]-4- bora-3a, 4a-diaza-*s*-indacene (F1)

1-heptyne (26.2 µL, 0.2 mmol), compound **4** (42.2 mg, 0.1 mmol), sodium ascorbate (4.0 mg, 20 mol %) and copper sulphate pentahydrate (2.5 mg, 10 mol %) were dissolved in 10 mL of ethanol-water mixture (7:3, v/v) and stirred for overnight. Saturated ammonium chloride solution was added to the reaction mixture (20 mL) and the crude product was extracted with dichloromethane. Then, crude product containing organic layer was dried over anhydrous sodium sulphate and purified on silica gel column chromatography. During the column chromatography purification, dichloromethane and hexane mixture (1:1, v/v) was used as an eluent initially. Then, polarity of the eluent mixture was progressively increased to dichloromethane: methanol (100:1, v/v) mixture. Evaporation of the combined organic phase yielded **F1** as red colored solid (Yield 44.8 mg, 73%).

HRMS ESI calculated for $C_{33}H_{43}BF_2N_9$ $[M+H]^+$: 614.3703; found: 614.3719. ^{1}H NMR ($CDCl_3$, 500 MHz): δ = 7.90 (s, 2H), 7.54 (d, J = 9.0 Hz, 2H), 7.22 (s, 2H), 7.02 (d, J = 4.0 Hz, 2H), 6.76 (d, J = 9.0 Hz, 2H), 6.56 (d, J = 1.5 Hz, 2H), 6.56 (d, J = 1.5 Hz, 2H), 4.41 (t, J = 6.0 Hz, 4H), 3.77 (t, J = 6.0 Hz, 4H), 2.68 (t, J = 8.0 Hz, 4H), 1.60-1.0 (m, 4H), 1.29-1.32 (m, 8H), 0.87 (t, J = 6.5 Hz, 6H). ^{13}C NMR ($CDCl_3$, 125 MHz): δ = 148.9, 148.5, 147.4, 142.7, 134.5, 133.2, 131.0, 123.6, 121.6, 118.0, 111.7, 51.4, 47.2, 31.4, 29.1, 25.5, 22.3, 13.9.

Synthesis of 4, 4-difluoro-8-[N, N-bis (2-(4-phenyl-1H-1, 2, 3-triazol-1-yl) ethyl) benzenamino]-4- bora-3a, 4a-diaza-*s*-indacene (F2)

Phenyl acetylene (22 µL, 0.2 mmol), compound **4** (42.2 mg, 0.1 mmol), sodium ascorbate (4.0 mg, 20 mol %) and copper sulphate pentahydrate (2.5 mg, 10 mol %) were dissolved in 10 mL of ethanol-water mixture (7:3, v/v) and stirred for overnight. Saturated ammonium chloride solution was added to the reaction mixture (15 mL) and reaction mixture was extracted with dichloromethane. Then, crude product was dried over anhydrous sodium sulphate and purified on silica gel column chromatography. Dichloromethane and hexane mixture (1:1, v/v) was used as eluent initially. Then, polarity of eluent mixture was gradually increased by using dichloromethane: methanol mixture (100:2, v/v). Red colored solid was obtained (Yield 43.2 mg, 69%). HRMS ESI calculated for $C_{35}H_{31}BF_2N_9$ $[M+H]^+$: 626.2764; found: 626.2784. ^{1}H NMR (DMSO-d6, 500 MHz): δ = 8.58 (s, 2H), 7.96 (s, 2H), 7.79 (d, J = 7.5 Hz, 4H), 7.42-7.45 (m, 6H), 7.32 (t, J = 7.0 Hz, 2H), 6.83-6.84 (m, 4H), 6.55 (dd, J= 3.0, 1.5 Hz, 2H), 4.66 (t, J = 5.5 Hz, 4H), 3.91 (t, J = 6.0 Hz, 4H). ^{13}C NMR (DMSO-d6, 125 MHz): δ = 150.6, 148.0, 147.0, 142.6, 133.9, 133.5, 131.1, 129.4, 128.4, 125.6, 122.7, 121.8, 118.7, 112.0, 50.0, 47.6.

Determination of Binding ratio and the apparent dissociation constant for the binding of Hg^{2+} ions to clickates (F1 and F2).

The binding ratio of BODIPY-Clickates and Hg^{2+} was determined by Job's continuation variation method. The fluorescence intensity was plotted against the mole fraction of clickates with total concentration of clickates and Hg^{2+} ions. Total concentration of

clickates and Hg^{2+} was 10 μM. Non-linear regression analysis was used to determine dissociation constant according to the equation **1** and the curve fitted with emission intensity against concentration of Hg^{2+}.[21] K_d is the apparent dissociation constant, n is binding ratio between Hg^{2+} and clickates. F_{min} is the fluorescence intensity in the absence of Hg^{2+}. F_{max} is fluorescence intensity of clickates with Hg^{2+}. F is the fluorescence intensity at any given Hg^{2+} with clickates.

$$F = (F_{max}[Hg^{2+}]^n + F_{min}K_d)/(K_d + [Hg^{2+}]^n) \quad \text{..... (1)}$$

Alamar blue assay

Lung adenocarcinoma (A549) cells was procured from NCCS, India. Resazurin was purchased from Sigma Aldrich, India. The A549 cells were grown in RPMI 1640 medium supplemented with 10% FBS (foetal bovine serum) at 37 °C and 5% CO_2. For Alamar blue assay, cells were seeded in 96 well plate as 8 $X10^3$ cells/well. After 24 hours, clickates mixed culture medium (5 to 40 μM) was added to the wells and incubated for 48 hours. The media was replaced with fresh media containing 10 % v/v of Alamar blue solution and incubated at 37 °C in dark for 1 hr. The media was taken out and change in the colour had been evaluated in multi-plate reader by taking absorbance at 570 nm to evaluate cell viability. All the experiments were performed in triplicates. Mean and standard error of mean had been calculated for each data set in GraphPad Prism software. Two tailed t-test had been performed to compare each dose with control with P = 0.05.

Cell culture

Bioimaging of Hg^{2+} was done in A549 cells. Cultured cells were cropped and seeded on 14 mm coverslips. After 24 hours post seeding on coverslips, cells were treated with 4 μL of 1 mM metal ions (final concentration: 2 μM) dissolved in sterilized phosphate buffer salined (PBS) at pH 7.4 and incubated for 30 min at 37 °C. Following that, the treated cells were washed with PBS three times to remove excess metal ions. Fluorescent probe supplemented in culture media (2 mL, final concentration: 2 μM) was added to the cell culture well. The samples were incubated at 37 °C for 30 min. Then, culture media was removed and cells were washed three times with PBS and coverslip were placed on glass slide for imaging. Fluorescence imaging was carried out with a ZEISS Axio Scope A1

Fluorescence Microscope with 545 nm excitation and 575-640 nm emission using a lamp (Hg 50 W).

Results and discussion

Synthesis

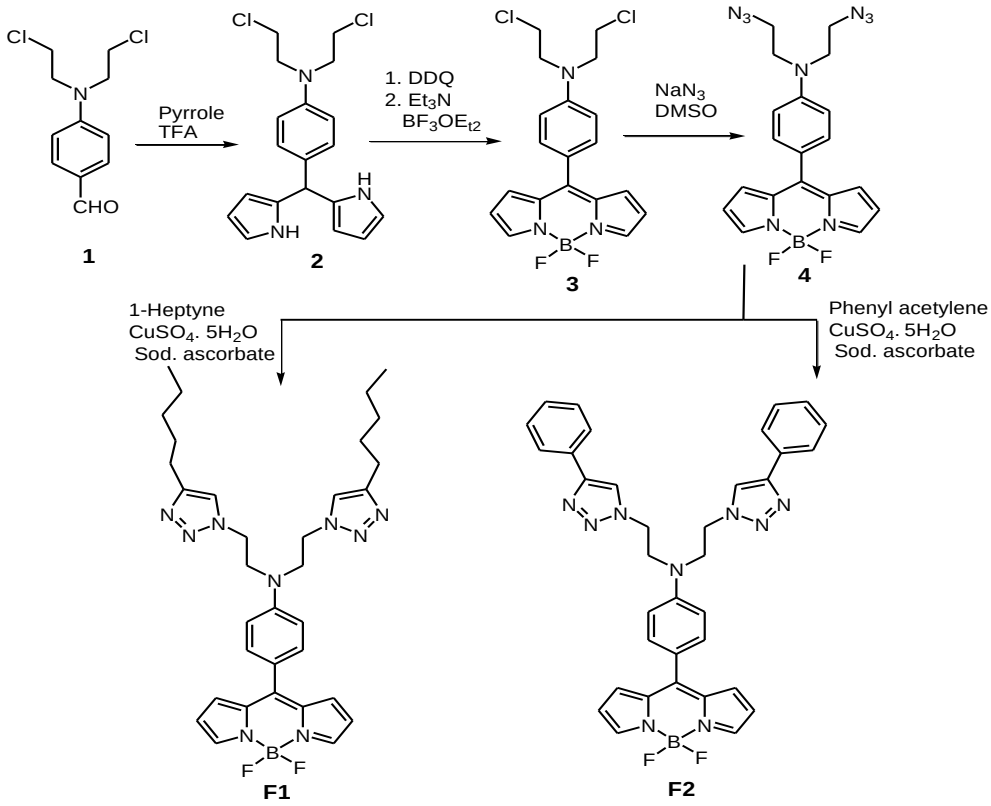

Scheme 1. Synthetic route of **F1** and **F2**.

We herein describe the Hg^{2+} sensing BODIPY based probes which had been synthesized utilizing click chemistry approach. As shown in scheme 1, the triazoles were attached to the *meso* substituted aromatic amine of fluorophores through ethylene spacers. Compound **1** was obtained using already reported procedure. Compound **2** had been synthesized by treating compound **1** with excess of pyrrole in the presence of trifluoroacetic acid under inert atmosphere. Dichloro-BODIPY derivative (**3**) was synthesized by subjecting compound **2** to oxidation and followed by addition of trimethylamine and boron trifluoride diethyl etherate. In next step, dichloro-BODIPY derivative was refluxed in acetonitrile with sodium azide to afford compound **4**. Click chemistry reaction of

compound **4** with 1-heptyne afforded **F1**, whereas **F2** was synthesized by the reaction between compound **4** and phenyl acetylene. All the compounds **1-4** were characterized by ^{1}H, ^{13}C NMR and HR mass spectrometry. The target molecules **F1** and **F2** were also characterized by 2D-NMR (^{1}H-^{1}H-COSY) techniques.

X-ray analysis

The single crystal X-ray structures of compounds **3** and **4** were determined and their ORTEP diagrams are given in figure 1. The crystal data refinement parameters for **3** and **4** are provided in ESI (Table **S2** and **S3**). The single crystals of compounds **3** and **4** were obtained by slow evaporation of the dichloromethane/n-hexane solution over a period of one week. Compound **3** (CCDC 10545488) gave orange platelet crystals having orthorhombic crystal system with $Pca2_1$ (#29) space group. Compound **4** (CCDC 1058841) gave orange needle shape crystals having monoclinic crystal system with $P2_1/c$ (#14) space group. The values of N-B-N angle were 105.83(17) and 105.82(14) respectively for compounds **3** and **4**. The values of F-B-F angle in compounds **3** and **4** were 109.79(18) and 108.8(15), respectively.

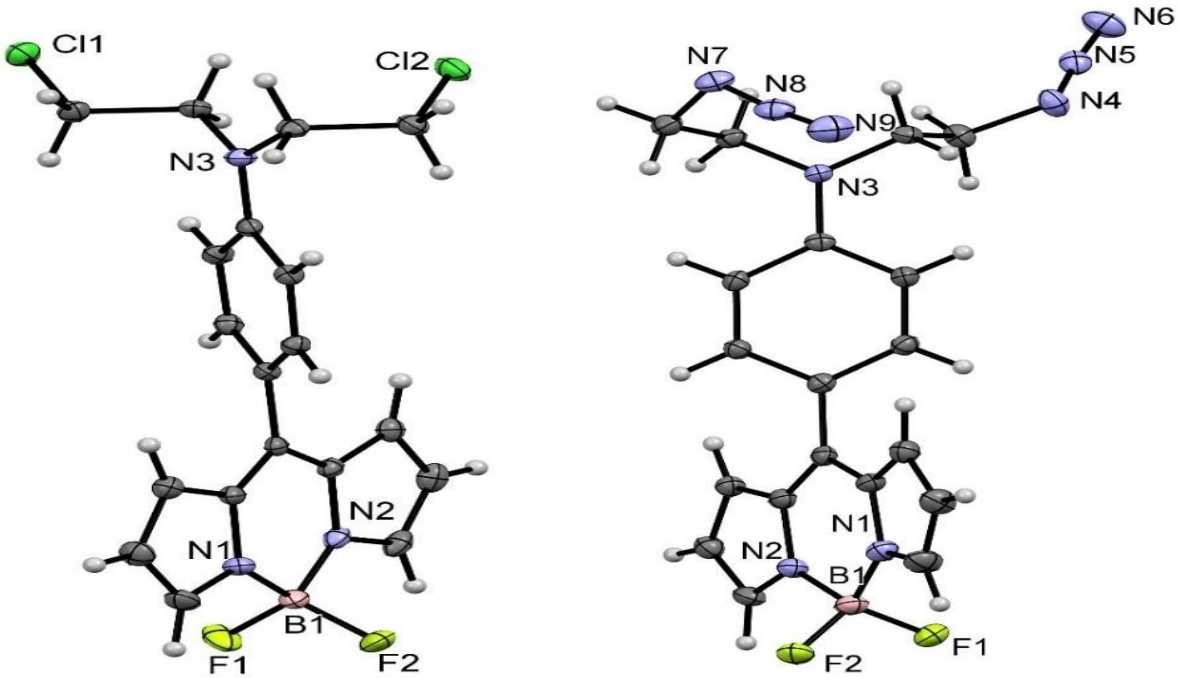

Figure 1. X-ray crystal structures of (a) compound **3** and (b) compound **4.** Thermal ellipsoids are shown at 50% probability level.

The C-Cl bond lengths in compound **3** were slightly higher [1.80(3) and 1.80(2) Å] than the typical value of 1.77 Å of C-Cl bond. In compound **4** the bond angles for azide groups: N4-N5-N9 and N7-N8-N9 were 173.15 ^{o} (18) and 172.12 ^{o} (18) respectively. Similar to the *meso*-phenyl substituted BODIPY the dipyrrins core of compounds **3** and **4** was essentially planar.[22] The substituted phenyl ring had perpendicular orientation with respect to the boron-dipyrrin plane. In compound **3** the dihedral angles between the boron dipyrrin units and the aryl ring (C4-C5-C10-C11, C6-C5-C10-C15) were 46.90 ^{o}(2) and 47.30^{o}(2) respectively. Similarly, in compound **4** the dihedral angles between the boron dipyrrin units and the aryl ring (C4-C5-C10-C15, C6-C5-C10-C11) were 59.40^{o}(3) and 51.10^{o}(3) respectively. The observed dihedral angles in both the compounds were comparatively lower than the previously reported *meso*-phenyl BODIPY[22] (dihedral angle, 60.80^{o}). The significantly lower value of dihedral angles in **3** and **4** suggested increased interactions between the boron-dipyrrin core and substituted phenyl ring in both the compounds.

Photophysical properties

The photophysical properties of BODIPY derivatives in different solvents were examined (Table S1). Compounds **3**, **4**, **F1** and **F2** showed an identical absorption profile around 490 to 500 nm, typical for **BODIPY** skeleton. This absorption peak could be assigned to the S_0-S_1 transition and had not been affected much due to solvent polarity. In contrast to absorption spectra, BODIPY derivatives exhibited solvent depended emission behaviour. In n-hexanes, these BODIPY derivatives emitted at green emission due to stabilization of locally excited (LE) state. New broad peak at red region was observed in tetrahydrofuran and dichloromethane as a result of intramolecular rotation induced charge transfer (CT). Fluorescence quantum yield of these derivatives was found to be relatively high in tetrahydrofuran than dichloromethane and the emission had been red shifted. Compound **3** and **4** have shown more red shifted emission with increasing solvent polarity over **F1** and **F2**. These findings suggested formation of two or more excited state conformers which might have resulted from intramolecular twist angle between *meso* phenyl ring and BODIPY, pyramidalization of aromatic amine nitrogen and dipole moment of solvent molecules.[23] Generally, solvent dependent TICT is less common in 1, 7-dimethyl and bulky group substituted BODIPY as steric hindrance control the intramolecular rotation.

No significant fluorescence signal was observed from both of LE and CT states in methanol, ethanol, acetonitrile and dimethyl formamide as ultra-fast charge transfer and other non-radiative quenching processes were dominant.[24] Visible and fluorescence pictures of compound **3**, **4**, **F1** and **F2** in different solvent have been provided in ESI (Figure S1).

Hg^{2+} sensing study

UV-visible spectrum of **F1** (λ_{abs} = 494 nm, € = 40,177 M^{-1} cm^{-1}) and **F2** (λ_{abs} = 494 nm, € = 52,322 M^{-1} cm^{-1}) in the absence of metal ions, exhibited an absorption band similar to the typical BODIPY dyes which indicated that absence of ground state interactions between triazoles and BODIPY.[25] **F1** (Φ_f = 0.002) and **F2** (Φ_f = 0.002) displayed very weak emission owing to the efficient energy transfer from the electron donating aromatic amine to the BODIPY skeleton. Fluorescence spectroscopy was used to mainly examine the emission of the clickates in the presence of metal cations. Clickates displayed a rapid and specific response to Hg^{2+} ions in methanol. As displayed in figure 2a and b, the emission intensity of both **F1** and **F2** were increased markedly only in the presence of Hg^{2+} ions (2-30 μM) in a concentration dependent manner accompanied by large Stokes shifts of 116 nm and 154 nm, respectively. In detail, upon addition of increasing amount of Hg^{2+} ions to the solution of **F1**, a remarkable fluorescence emission band centred at 620 nm was observed. Coordination of Hg^{2+} with **F2** had caused a new enhanced broad structure less emission band around 660 nm. In a sharp contrast to typical PET based BODIPY probes,[26] these clickates exhibited metal ion induced emission band around 620 to 660 nm. Spectral shift could be possible if Hg^{2+} had brought the clickates from the LE state to the CT state through intramolecular rotation. Bathochromically shifted emission spectra confirmed the excited state reaction that led to the formation of new species, which might conformationally different from the ground state species.[27] Nature of the cation, size of the cavity, binding manner of cation to the receptor hetero atoms and solvent molecule could have pronounced influence on intramolecular rotation.[28] These observations suggested formation *endo* complex conformer which could be different from recently reported triazole based metal ion probes.[19a, 29] Though coordination of heavy metal ions with organic luminescence probes predominately resulted fluorescence

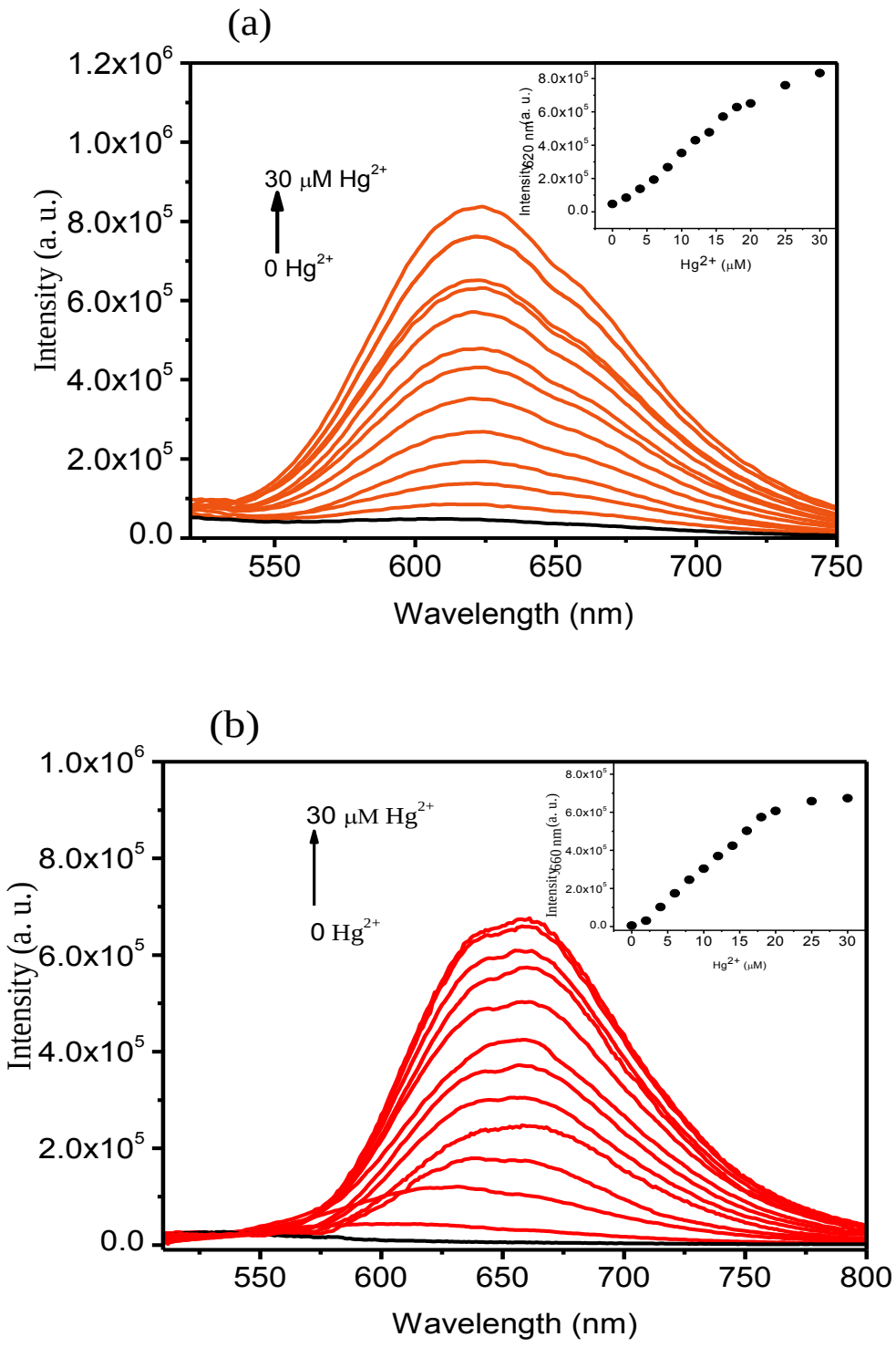

Figure 2. Fluorescence response of (a) **F1** (10 μM) and (b) **F2** (10 μM) in the presence of different amounts of Hg^{2+} in methanol (λ_{ex} = 494 nm); Inset: The relationship between maximum fluorescence intensity of **F1** or **F2** with increasing concentrations of Hg^{2+}.

quenching, conformationally favourable clickates-Hg^{2+} complexes could neglect the spin-orbit coupling and could form the distinct excited state conformers. This sensing mechanism is similar to already reported metal ion induced CT probes.[30] In the presence of 3 equivalent of Hg^{2+}, fluorescence enhancement of 36 fold and 27 fold were achieved by the clickates **F1** (Φ_f = 0.072) and **F2** (Φ_f = 0.054), respectively. The metal ions selectivity test of clickates was evaluated by mixing them with 3 equivalents of Ag^{+}, Ca^{2+}, Cd^{2+}, Co^{2+}, Cu^{2+}, Fe^{3+}, Fe^{2+}, K^{+}, Mg^{2+}, Mn^{2+}, Ni^{2+}, Pb^{2+}, and Zn^{2+}. Clickates had shown high selectivity towards Hg^{2+} over other metal ions. Even chemically similar cations such as Ag^{+}, Cd^{2+}, Cu^{2+}, and Pb^{2+} did not have significant effect on clickate's emission intensity (figure 3 and S2).

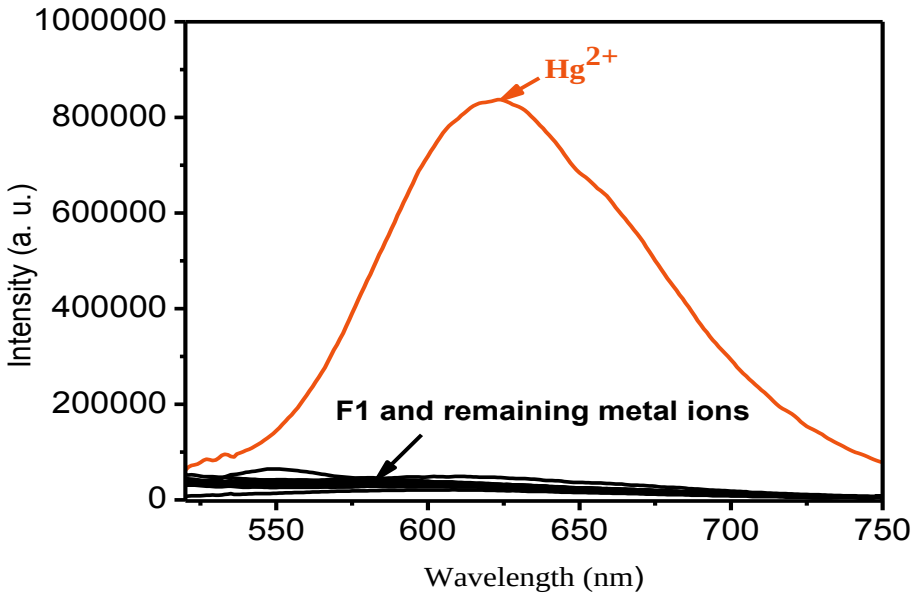

Figure 3. Fluorescence spectra of **F1** (10 µM) upon addition of 3 equivalent of various metal ions (Ag^{+}, Ca^{2+}, Cd^{2+}, Co^{2+}, Cu^{2+}, Fe^{3+}, Fe^{2+}, K^{+}, Mg^{2+}, Mn^{2+}, Ni^{2+}, Pb^{2+}, Zn^{2+} and Hg^{2+} in methanol (λ_{ex} = 494 nm).

Almost no changes were observed on absorption profile of clickates upon addition of 3 equivalents of Ag^{+}, Ca^{2+}, Cd^{2+}, Co^{2+}, Cu^{2+}, Fe^{3+}, Fe^{2+}, K^{+}, Mg^{2+}, Mn^{2+}, Ni^{2+}, Pb^{2+}, and Zn^{2+} (figure 4 and S3). The absorption band of **F1** centered at 494 nm gradually shifted to 501 nm with the increasing addition of Hg^{2+}, indicated that aromatic amine and two triazoles were participated in the chelation event (figure S4a). Similar to **F1**, absorption

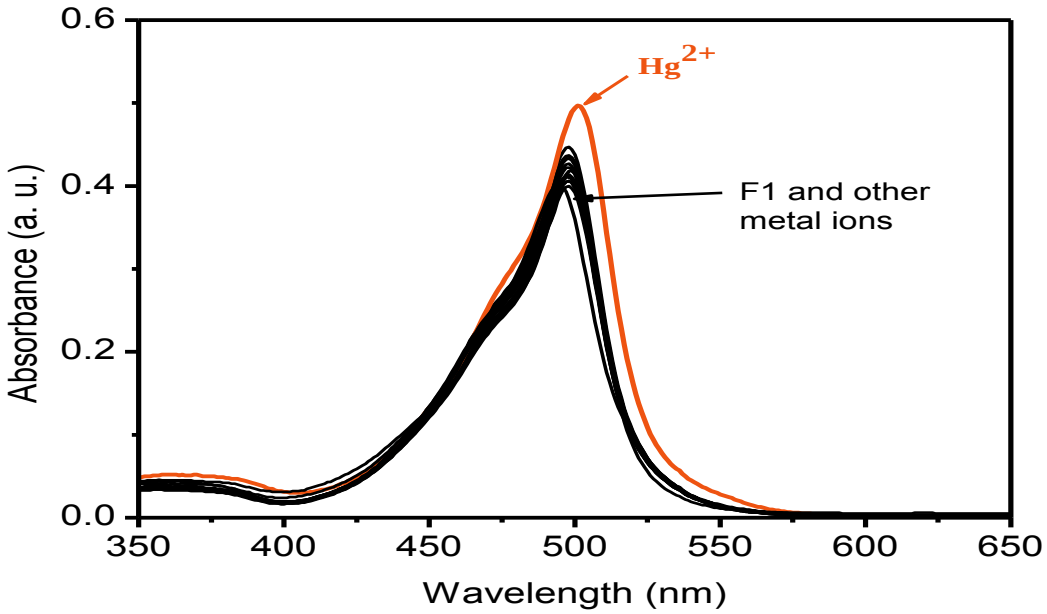

Figure 4. UV-visible spectra of **F1** (10 μM) upon addition of 3 equivalent of various metal ions (Ag^{+}, Ca^{2+}, Cd^{2+}, Co^{2+}, Cu^{2+}, Fe^{3+}, Fe^{2+}, K^{+}, Mg^{2+}, Mn^{2+}, Ni^{2+}, Pb^{2+}, Zn^{2+} and Hg^{2+} in methanol.

band of **F2** centered at 494 nm steadily shifted to 506 nm with addition of Hg^{2+} (figure S4b). The apparent dissociation constant was determined by non-linear regression analysis from Hg^{2+} ion titration curve and found to be 24.4 ± 5.1 μM and 22.0 ± 3.9 μM for **F1** and **F2** (figure S5a and b), respectively. Limit of detection for the detection of Hg^{2+} was found to be 5.1 nM and 7.2 nM at the signal to noise ratio S/N = 3 for **F1** and **F2**, respectively.

Competitive test and binding ratio

Competitive test were performed to study the effect of interference from other metal ions (figure 5 and S6). 15 equivalent of appropriate metal ions were mixed with clickates (10 μM) and Hg^{2+} ions (3 equiv.) were added to solution subsequently. Hg^{2+} induced enhanced emission of clickates did not change significantly even in the presence of excess of other metal ions because of binding mode was highly specific and highly sensitive towards Hg^{2+}. Job plot suggested that both **F1** and **F2** formed a 1:1 complex with Hg^{2+} ion (figure 6 and S7), individually. In ESI-MS spectra, peaks at m/z 816.51 and 827.44 were assigned to **F1-Hg^{2+}** and **F2-Hg^{2+}** complexes (figure S8a and b), respectively. All above findings proved that BODIPY based clickates could sense Hg^{2+} ions both qualitatively and quantitatively.

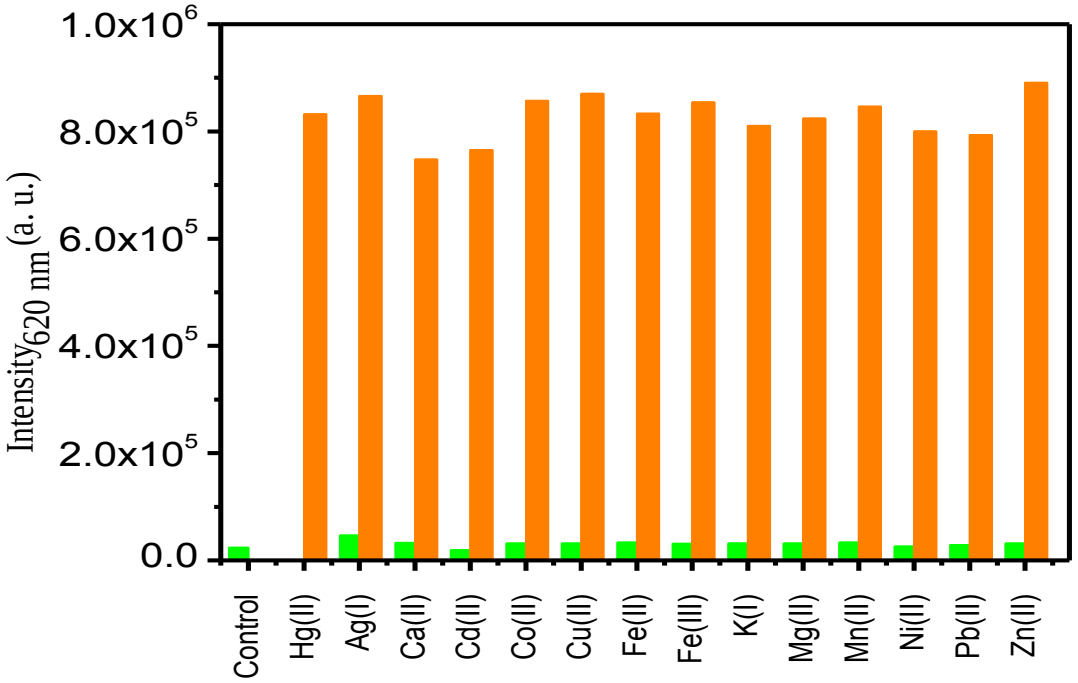

Figure 5. Relative fluorescence intensities of **F1** (10 μM) and in the presence of Hg^{2+} (3 equiv.) and various metal ions (15 equiv.) in methanol, (λ_{ex} = 494 nm). Green bars represent **F1** and 150 μM of other competing metal ions; saffron bars represent subsequent addition of 30 μM of Hg^{2+} to **F1** and **F1**with competing metal ions (150 μM).

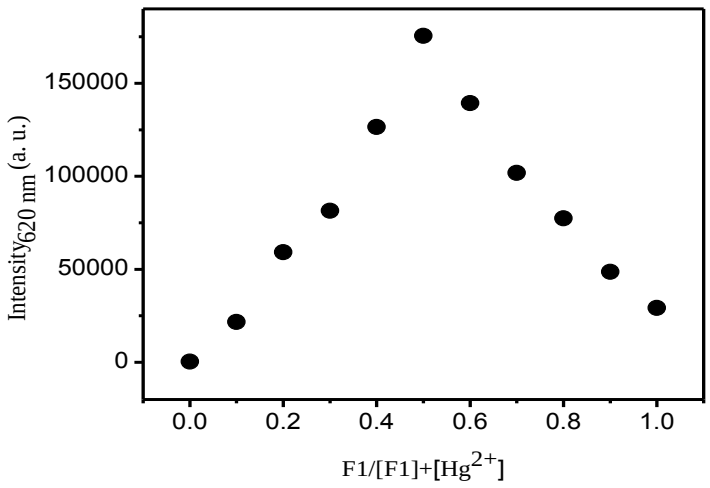

Figure 6. Job plot of **F1-Hg^{2+}** complexes in methanol (λ_{ex} = 494 nm). The total concentration of **F1** and Hg^{2+} was 10 μM.

Effect of pH

Emission intensity of clickates was very low in a tested pH range and indicated insensitivity on presence of hydrogen ion concentration. As illustrated in figure 7 and S9,

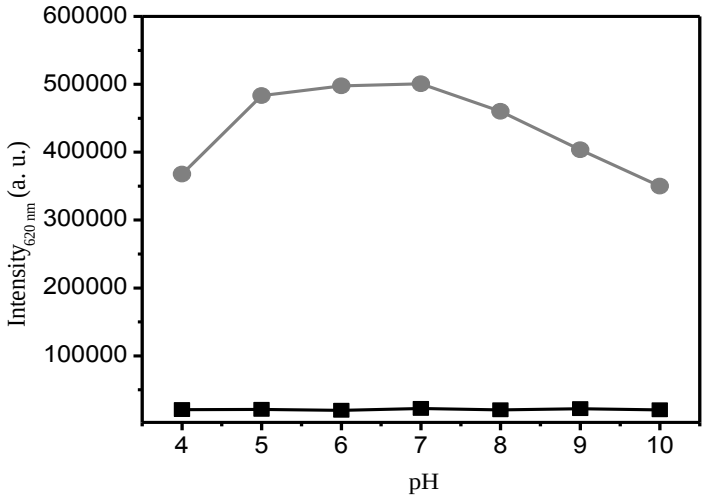

Figure 7. Fluorescence intensity of **F1** (10 μM; ■) and after addition of Hg^{2+} (30 μM, ●) in methanol-water (9:1, v/v, 2 mM HEPES) medium as a function of different pH values. Excitation wavelength was 494 nm.

both clickates could sense Hg^{2+} in the most common pH range of 4-10. Moreover, Hg^{2+} induced emission was almost stable in biologically significant pH range of 5 to 8. Both high and low pH range, fluorescence intensity was relatively low which could be attributed to unstable nature of triazole-Hg^{2+} complex at this pH range.

NMR titration

Next, NMR spectroscopy was used to examine Hg^{2+} binding sites in clickates as metal ion binding could alter proton signals close to binding sites. In a typical manner, proton NMR spectra were acquired in DMSO-d6 by gradually increasing the concentration of Hg^{2+} to the clickates. In case of **F1** (figure 8), triazole proton at δ 7.86 and methylene protons at δ 4.51, 3.76, and 2.56 were downfielded to δ 7.99, 4.55, 3.78 and 2.60 upon addition of 2 equivalent of Hg^{2+}. Aromatic protons (δ 6.85) were slightly upfielded to δ 6.80. From the NMR spectra, we concluded that downfield shift of triazole proton and methylene protons had taken place due to effective binding process. In contrast to **F1**, coordination of Hg^{2+} with **F2** had changed chemical shifts of binding cite's neighbour protons very slightly.

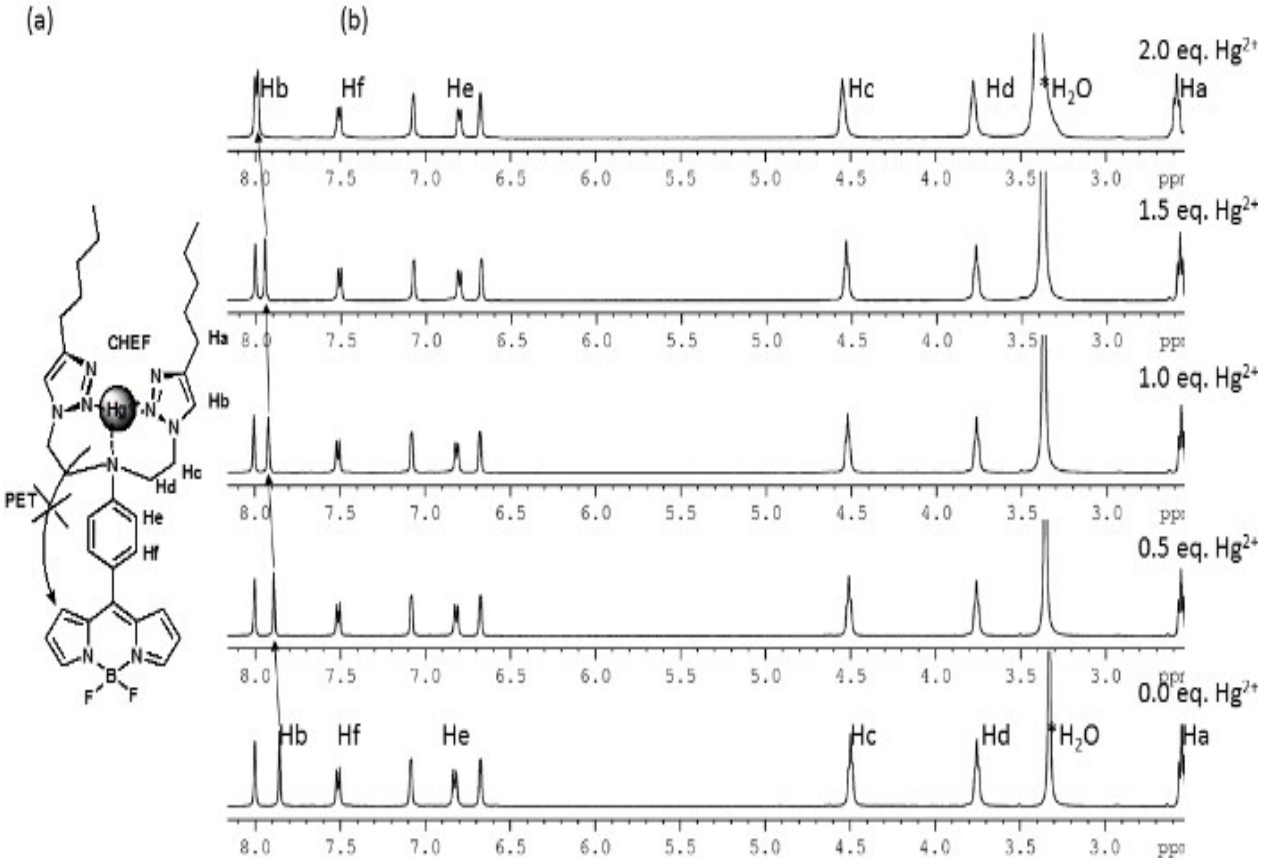

Figure 8. (a) Binding model (b) Partial ^{1}H NMR spectra of **F1** (5mM) in the absence or presence of increasing Hg^{2+} in DMSO-d6.

protons. As depicted in **F2** (figure S10 a and b), phenyl group, triazole and aromatic amine were involved in the binding event. Phenyl group protons at δ 7.41-7.45 (m) were shifted to δ 7.38-7.44 (m). Triazole and methylene protons chemical shift were also slightly upfielded.

Cytotoxicity and bioimaging studies

Cytotoxicity of clickates was evaluated using alamar blue assay after exposure of A549 cells to a concentration range of 0 – 40 µM for 48 hours. The results showed that after 48 hours of treatment of **F1**, at all concentrations nearly ≥85% cells were viable, showing no significant cell death. The difference between cell proliferation rate of all the concentration and control was evaluated as to be non-significance at 95% confident

interval. The **F2** viability data had showed more biocompatibility with more than 95% cell viability at all the concentrations. These data clearly indicated excellent biocompatibility of these clickates for biological applications (figure 9). The title compounds were internalized into the cells possibly by receptor mediated endocytosis.[31] Fluorescence imaging showed the internalization of clickates in A549 cells after Hg^{2+} treatment (figure 10).

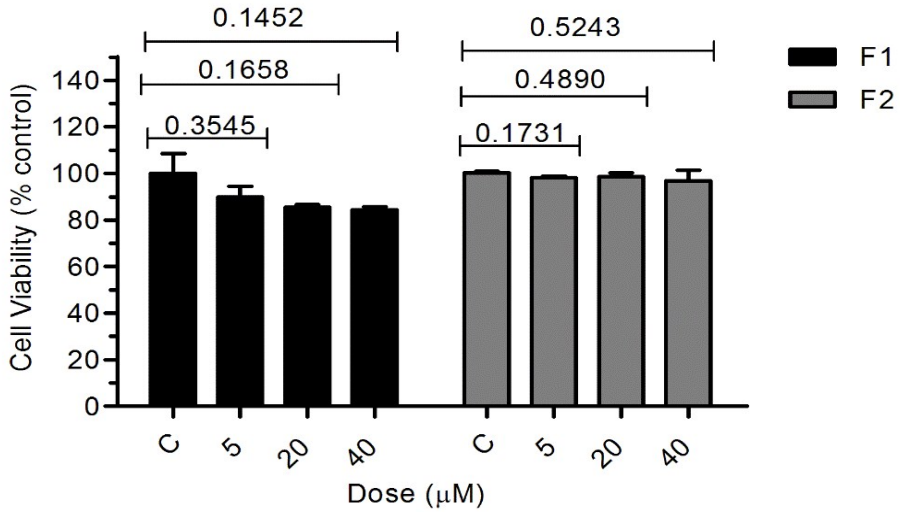

Figure 9. Cell viability test of **F1** and **F2** in A549 cells. The values showing above the bars indicating P values between control and each concentration dose of clickates

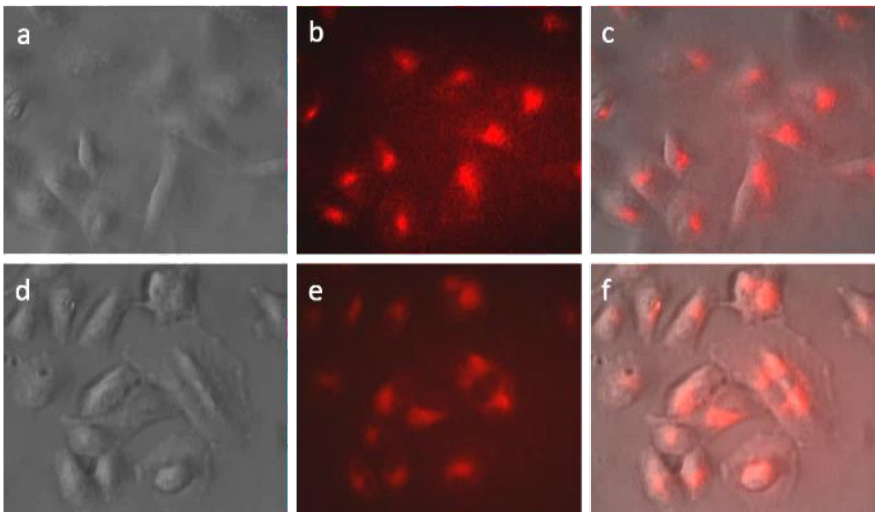

Figure 10. Fluorescence imaging of Hg^{2+} ion (2 μM) using clickates (2 μM) in live A549 cells. Upper panel shows **F1** and lower panel shows **F2** internalized A549 cells. (a and d) bright field images, (b and e) fluorescent images, (c and f) merged images.

The bright fluorescence and overlaid images displayed intra-cellular localization of fluorescence signals in A549 cells, indicated a cytoplasmic distribution of Hg^{2+} and cell membrane permeability of **F1** and **F2**.

Conclusion

In conclusion, we have demonstrated the prospective and the versatility of triazoles functionalized BODIPY for the detection of Hg^{2+}. Both clickates exhibited the high selectivity towards Hg^{2+} over other competing metal ions with large Stoke shifts through charge transfer mechanism. This methodology is not limited to Hg^{2+} sensing but can also be applied to design red light emitting fluorescent probes for other metal ions.

Acknowledgements

IG gratefully acknowledges CSIR (Govt. of India) and IIT Gandhinagar for financial support. IG thanks Prof. H. Furuta, Kyushu University for X-ray analysis. MV thanks IIT Gandhinagar for post-doctoral fellowship. RV acknowledges DST (Govt. of India) and Gujarat State Biotechnology Mission (Govt. of Gujarat) for the financial support. DK thanks Department of Biotechnology (Govt. of India) for research fellowship.

References

1. (a) S. Ekino, M. Susa, T. Ninomiya, K. Imamura and T. Kitamura, *J. Neurol. Sci.*, 2007, **262**, 131; (b) J. R. Wands, S. W. Weiss, J. H. Yardley and W. C. Maddrey, *Am. J. Med.*, 1974, **57**, 92; (c) T. W. Clarkson, *Environ. Health Persp.*, 1993, **100**, 31; (d) J. T. Salonen, K. Seppänen, K. Nyyssönen, H. Korpela, J. Kauhanen, M. Kantola, J. Tuomilehto, H. Esterbauer, F. Tatzber and R. Salonen, *Circulation*, 1995, **91**, 645.
2. (a) O. S. Wolfbeis, *J. Mater. Chem.*, 2005, **15**, 2657; (b) J. L. West and N. J. Halas, *Annu. Rev. Biomed. Eng.*, 2003, **5**, 285.
3. (a) S.-Y. Moon, N. J. Youn, S. M. Park and S.-K. Chang, *J. Org. Chem.*, 2005, **70**, 2394; (b) A. Pariyar, S. Bose, S. S. Chhetri, A. N. Biswas and P. Bandyopadhyay, *Dalton Trans.*, 2012, **41**, 3826; (c) H. Lee, H.-S. Lee, J. H. Reibenspies and R. D. Hancock, *Inorg. Chem.*,

2012, **51**, 10904; (d) D. S. McClure, *J. Chem. Phys.*, 1949, **17**, 665; (e) S. Y. Moon, N. R. Cha, Y. H. Kim and S.-K. Chang, *J. Org. Chem.*, 2004, **69**, 181.

4. (a) N. Boens, V. Leen and W. Dehaen, *Chem. Soc. Rev.*, 2012, **41**, 1130; (b) T. Kowada, H. Maeda and K. Kikuchi, *Chem. Soc. Rev.*, 2015, **44**, 4953; (b) S. Madhu, D. K. Sharma, S. K. Basu, S. Jadhav, A. Chowdhury and M. Ravikanth *Inorg. Chem.*, 2013, **52**, 11136.

5. (a) K. P. Carter, A. M. Young and A. E. Palmer, *Chem. Rev.*, 2014, **114**, 4564; (b) M. J. Culzoni, A. Munoz de la Pena, A. Machuca, H. C. Goicoechea and R. Babiano, *Anal. Methods*, 2013, **5**, 30.

6. (a) G. M. Cockrell, G. Zhang, D. G. VanDerveer, R. P. Thummel and R. D. Hancock, *J. Am. Chem. Soc.*, 2008, **130**, 1420; (b) N. C. Lim, J. V. Schuster, M. C. Porto, M. A. Tanudra, L. Yao, H. C. Freake and C. Brückner, *Inorg. Chem.*, 2005, **44**, 2018.

7. S. Goswami, K. Aich, S. Das, C. Das Mukhopadhyay, D. Sarkar and T. K. Mondal, *Dalton Trans.*, 2015, **44**, 5763.

8. S. H. Kim, H. S. Choi, J. Kim, S. J. Lee, D. T. Quang and J. S. Kim, *Org. Lett.*, 2010, **12**, 560.

9. S. Sinha, R. R. Koner, S. Kumar, J. Mathew, M. P. V, I. Kazi and S. Ghosh, *RSC Adv.*, 2013, **3**, 345.

10. (a) W. Rettig, *Angew. Chem. Int. Ed. Engl.*, 1986, **25**, 971. (b) A. Nakamura, S. Sato, K. Hamasaki, A. Ueno and F. Toda, *J. Phys. Chem.*, 1995, **99**, 10952. (c) M. Maus and W. Rettig, *J. Phys. Chem. A*, 2002, **106**, 2104. (d) K. Rurack, W. Rettig and U. Resch-Genger, *Chem. Commun.*, 2000, 407.

11. (a) K. Rurack, U. Resch, M. Senoner and S. Dahne, *J. Fluoresc.*, 1993, **3**, 141. (b) J. Herbich, Z. R. Grabowski, H. Wojtowicz, K. Golankiewicz, *J. Phys. Chem*, 1989, **93**, 3439.

12. J. J. Bryant and U. H. F. Bunz, *Chem. Asian J.*, 2013, **8**, 1354.

13. J. John, J. Thomas and W. Dehaen, *Chem. Commun.*, 2015, **51**, 10797.

14. D. Astruc, L. Liang, A. Rapakousiou and J. Ruiz, *Acc. Chem. Res.*, 2012, **45**, 630.

15. C.-Z. Ruan, R. Wen, M.-X. Liang, X.-J. Kong, Y.-P. Ren, L.-S. Long, R.-B. Huang and L.-S. Zheng, *Inorg. Chem.*, 2012, **51**, 7587.

16. (a) D. Maity and T. Govindaraju, *Chem. Commun.*, 2012, **48**, 1039; (b) M. Vedamalai and S.-P. Wu, *Org. Biomol. Chem.*, 2012, **10**, 5410; (c) E. Ganapathi, S. Madhu and M. Ravikanth, *Tetrahedron*, 2014, **70**, 664.

17. E. M. Sletten and C. R. Bertozzi, *Angew. Chem. Int. Ed. Engl.*, 2009, **48**, 6974.
18. I. L. Lee, Y.-M. Sung and S.-P. Wu, *RSC Adv.*, 2014, **4**, 25251.
19. (a) M. Vedamalai and S. P. Wu, *Eur. J. Org. Chem.*, 2012, **2012**, 1158; (b) R. S. Singh, R. K. Gupta, R. P. Paitandi, A. Misra and D. S. Pandey, *New J. Chem.*, 2015, **39**, 2233.
20. Morgan, P. Bagchi and C. J. Fahrni, *J. Am. Chem. Soc.*, 2011, **133**, 15906.
21. S. C. Dodani, Q. He, and C. J. Chang, *J. Am. Chem. Soc.*, 2009, **131**, 18020.
22. H. L. Kee, C. Kirmaier, L. Yu, P. Thamyongkit, W. J. Younblood, M. E. Calder, L. Ramos, B. C. Noll, D. B. Bocian, R. Scheidt, R. R. Brige, J. S. Lindsey and D. Holten, *J. Phys. Chem. B.* 2005, **109**, 20433.
23. R. Hu, E. Lager, A. Aguilar-Aguilar, J. Liu, J. W. Y. Lam, H. H. Y. Sung, I. D. Williams, Y. Zhong, K. S. Wong, E. Pena-Cabrera, and B. Z. Tang, *J. Phys. Chem. C*, 2009, **113**, 15845.
24. (a) M. Kollmannsberger, K. Rurack, U. Resch-Genger and J. Daub, *J. Phys. Chem. A*, 1998, **102**, 10211. (b) R. Hu, C. F. A. Gomez-Duran, J. W. Y. Lam, J. L. Belmonte-Vazquez, C. Deng, S. Chen, R. Ye, E. Pena-Cabrera, Y. Zhong, K. S. Wong, and B. Z. Tang, *J. Phys. Chem. C*, 2009, **113**, 15845.
25. A. Loudet and K. Burgess, *Chem, Rev.*, 2007, **107**, 4891.
26. (a) J. Wang and X. Qian, *Org. Lett*., 2006, **8**, 3721. (b) B. Sui, S. Tang, T. Liu, B. Kim and K. D. Belfield, *ACS Appl. Mater. Interfaces*, 2014, **6**, 18408.
27. (a) K. Rurack, M. Kollmannsberger, U. Resch-Genger and J. Daub, *J. Am, Chem, Soc*., 2000, **122**, 968.
28. Z. R. Grabowski, K. Rotkiewicz and W. Rettig, *Chem. Rev*., 2003, **103**, 3899.
29. W.-J, Shi, J.-Y. Liu, and D. K. P. Ng, *Chem. Asian. J*., 2012, **7**, 196.
30. (a) S. Aoki, D. Kagata, M. Shiro, K. Takeda and E. Kimura, *J. Am. Chem. Soc.*, 2004, **126**, 13377. (b) L. Xue, C. Liu and H. Jiang, *Org. Lett.*, 2009, **11**, 1655.
31. D. Soulet, L. Covassin, M. Kaouass, R. Charest-Gaudreault, M. Audette and R. Poulin, *Biochem. J.*, 2002, **367**, 347.

Manuscript: *Design and synthesis of BODIPY-Clickates based Hg^{2+} sensors: Effect of triazole binding mode with Hg^{2+} on signal transduction*

Manuscript number: DT-ART-10-2015-004042

Graphical Abstract

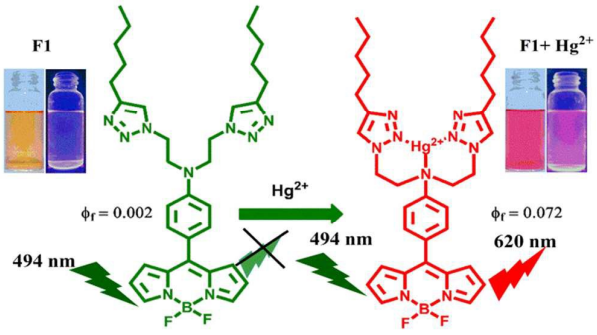

Highly selective BODIPY-Clickates for mercury sensing are reported. These BODIPY Clickates exhibits emission in red region with unprecedented large Stokes shifts (116 and 154 nm) upon mercury ion binding due to the intramolecular charge transfer processes.